ANALYSIS OF GYROSCOPIC EFFECTS IN ROTOR-DISC SYSTEMS

D.VENKATARAMANAIAH M.Tech (M.D), AHTC Student, Mech Engg Dept
E-Mail: dvr_in86@gmail.com

B.T.NAIK M.Tech (Ph.D)
Associate Prof., Mech Engg Dept (HOD)
In AHTC, Hyd, T.S., India.
E-Mail:btnaik96@gmail.com

ABSTRACT

This work deals with study of dynamics of a viscoelastic rotor shaft system, where Stability Limit of Spin Speed (SLS) and Unbalance Response amplitude (UBR) are two indices. The Rotor Internal Damping in the system introduces rotary dissipative forces which is tangential to the rotor orbit, well known to cause instability after certain spin speed. There are two major problems in rotor operation, namely high transverse vibration response at resonance and instability due to internal damping. The gyroscopic stiffening effect has some influence on the stability. The gyroscopic effect on the disc depends on the disc dimensions and disc positions on the rotor. The dynamic performance of the rotor shaft system is enhanced with the help of gyroscopic stiffening effect by optimizing the various disc parameters (viz. disc position and disc dimension). This optimization problem can be formulated using Linear Matrix Inequalities (LMI) technique. The LMI defines a convex constraint on a variable which makes an optimization problem involving the minimization or maximization of a performance function belong to the class of convex optimization problems and these can incorporate design parameter constraints efficiently. The unbalance response of the system can be treated with $H\infty$ norm together with parameterization of system matrices. The system matrices in the equation of motion here are obtained after discretizing the continuum by beam finite element. The constitutive relationship for the damped beam element is written by assuming a Kelvin – Voigt model and is used to obtain the equation of motion. A numerical example of a viscoelastic rotor is shown to demonstrate the effectiveness of the proposed technique.

INTRODUCTION

Flexible mechanical systems are gaining an increasing significance as more large- scale machinery is being built. The majority of modern machines incorporate some form of flexible rotor-bearing system in order to control and distribute mechanical power and many of these include propeller attachments. Examples include wind turbines, marine propulsion systems and turbo machinery. Current design trends for rotating equipment aim to heighten efficiency by reducing weight and increasing operating speeds. These goals are being made more attainable by a greater understanding of rotor-dynamic behaviour and improved methods for predicting system responses. The ground theory of mechanisms and machines dates back to the early twentieth century, but the dynamic analysis of flexible mechanisms is often too complex for an analytical solution. Thus it is with the increased power of modern computers that new methods of behaviour prediction are being developed for flexible mechanisms.

Vibration analysis is essential in the design and analysis of rotating machinery. The majority of vibrations are caused by rotation related sources of some description, (normally imbalance) consequently the forces are synchronous to the rotational speed. Thus, forced vibration analysis is fundamental in the design and analysis of rotating machinery. The two most commonly used methods of forced frequency analysis are the finite element, or transfer matrix method. However since certain effects (including, gyroscopic, centrifugal stiffening, and fluid bearings) are dependant on the rotational speed the methods require computational assembly and inversion of large matrices at each frequency step. This is computationally expensive and inefficient however with the advances in modern computing speed it is rapidly becoming less of a problem.

The transfer matrix approach allows for a continuous representation of the shaft system and produces results in good agreement to experimental work. Its main advantage is the small amount of computer memory and power required to analyse systems. However, the equations of motion are not explicitly written and some experimental work is usually required in obtaining the transfer matrices. Therefore, as computers have become exponentially more powerful, finite element methods are now largely replacing those based on transfer matrices. This is especially true during initial system design stages when transfer matrices may be difficult to verify.

The finite element method provides a methodical approach for the discretization of a continuum. It can provide a solution for many types of complicated systems including fluid flows, heat exchange, static mechanical stresses, or dynamic mechanical systems, including those examined in this study.

OVERVIEW OF AVAILABLE LITERATURE

Rotordynamic studies related to technological applications date back to the second half of the nineteenth century, when the increase of the rotational speed of many machine elements made it necessary to include rotation into the analysis of their dynamic behaviour. However, the dynamics of rotating systems, as far as rigid rotors are concerned, was already well understood and the problem of the behaviour of the spinning top had been successfully dealt with by several mathematicians and theoretical mechanicists.

The paper which is considered to be the first paper fully devoted to Rotordynamics is, on the centrifugal force on rotating shafts, published in The Engineer by Rankine [29]. It correctly states that a flexible rotating system has a speed, defined by the author as critical speed, at which very large vibration amplitudes are encountered. However, the author incorrectly predicts that stable running above the critical speed is impossible.

Earlier attempts to build turbines, mainly steam turbines, at the end of nineteenth century led to rotational speeds far higher than those common in other fields of mechanical engineering. At these speeds, some peculiar dynamic problems are usually encountered and must be dealt with to produce a successful design. De Laval had to solve the problem correctly understanding the behaviour of a rotor running at speeds in excess of critical speed, i.e., in supercritical conditions, while designing his famous cream separator and then his steam turbine.

A theoretical explanation of supercritical running was supplied first by Foppl [21], Belluzzo [9], Stodola [6] and Jeffcott [25] in his famous paper of 1919. Although the first turbine rotors were very simple and could be dealt with by using simple models, of the type now widely known as Jeffcott rotor, more complex machines required a more detailed modelling. Actually, although a simplified approach like the above-mentioned Jeffcott rotor can explain qualitatively many important features of real-life rotors, the most important being self-centring in supercritical conditions and the different roles of the damping of the rotor and of the nonrotating parts of the machine, it fails to explain other features, such as the dependence of the natural frequencies on the rotational speed. Above all, the simple Jeffcott rotor does not allow us to obtain a precise quantitative analysis of the dynamic behaviour of complex systems, e.g., those encountered in gas or steam turbines, compressors, pumps, and many other types of machines.

ROTOR SYSTEM MODELLING AND OPTIMISATION

The foundation of analysis is laid here. This chapter includes the Finite Element Modelling of a rotor system followed by optimisation of various disc parameters ensuring high stability of the system.
Here the rotor-bearing system is considered to comprise a set of interconnecting components consisting of rigid discs, rotor segments with distributed mass and elasticity, and linear bearings. In this section the rigid disc equation of motion is developed using a Lagrangian formulation. The finite rotor element equation of motion is developed in an analogous manner by specifying spatial shape functions and then treating the rotor element as an integration of an infinite set of differential discs. The bearing equations are not developed and only the linear forms of the equations are utilized in this work.

RESULTS AND DISCUSSIONS

This section involves a design of a solid rotor disc mounted on a rotor shaft as shown in the Figure (). The rotating shaft is supported by bearings at both ends and assumed to be as damped support. The stiffness and the damping effects of the bearing supports are simulated by springs and viscous dampers (k_{yy} = 70 MN/m, k_{zz} = 50 MN/m, d_{yy} = 700 Ns/m and d_{zz} = 500Ns/m) in the two transverse directions. Following Lalanne and Ferraris [4], the material properties of the steel rotor are shown in Table (). The purpose is to design the rotor shaft system in order to ensure low unbalance response amplitude (UBR) and high stability limit of spin speed (SLS). The design variables chosen here are the diameter and thickness of a disc and its position on the system. The initial diameter and thickness and the unbalance on the disc are shown in Table (). The problem involves proper placement of various discs on the rotor shaft system and at the same time to represent the techniques of optimization of various design parameters of the disc for achieving the better gyroscopic stiffening effect. The sole purpose of this study is to represent techniques of optimisation of various parameters of a rotor-shaft-disc system and therefore, to obtain high stability and no feasibility study has been done on the results so obtained.

Material	Density (kg/m^3)	Young's Modulus (GPa)	Length(m)	Diameter(m)	Damping Coefficient (N-s/m)
Mild Steel	7800	200	1.3	0.2	0.0002

Table : Rotor Material and its Properties.

Diameter(m)	0.20
Thickness(m)	0.05
Mass Unbalance(kg-m)	2e-3

Table : Disc parameters

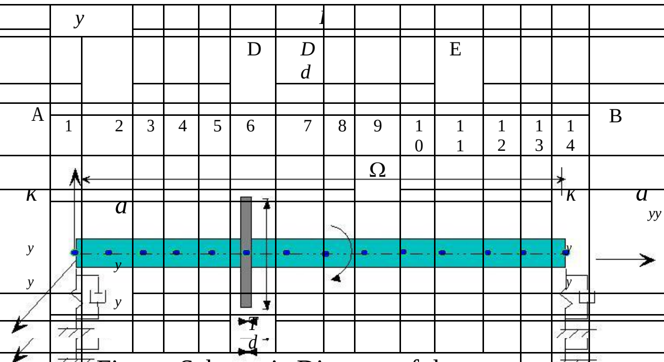

Figure Schematic Diagram of the Rotor shaft system

Rotor shaft system

DISC POSITIONS

The material damping in the rotor shaft introduces rotary dissipative forces which is tangential to the rotor orbit, well known to cause instability after certain spin speed (Zorzi and Nelson [34]). Thus high speed rotor operation suffers from two problems viz. 1) high transverse response due to resonance and 2) instability of the rotor-shaft system over a spin-speed. Both phenomena occur due to material inherent properties and set limitations on operating speed of rotor. By using light weight and strong rotor, the rotor operating speed can be enhanced. These two parameters have some practical limitation. In other words the gyroscopic stiffening effect has some influence on the stability. The gyroscopic effect on the disc depends on the disc dimension and disc position on the rotor. Thus, the optimum positioning of the discs may achieve high speeds and maximum stability. The proper positioning helps ensure high SLS. SLS of the rotor–shaft system has been found out from the maximum real part of all eigenvalues. The system becomes unstable when the real part touches the zero line.

The various disc positions for a single disc rotor are the consecutive nodes. But obtaining the different sets of disc position for a multi disc rotor is not straight forward. It has been done by performing the permutation between the total number of nodes and total number of disc. So the total sets of disc position for a simply supported rotor are given by $N \square {}^{n}P_{j}$, where n+2 are the total number nodes and j is the no. of discs.

The plots for SLS are found to be symmetric about the vertical axis and it can be seen that the maximum SLS is obtained when the discs are towards the ends of the rotor and if the discs are more towards the centre of the rotor then minimum SLS is obtained. In other words, the rotor will be more stable if the discs are placed towards the ends of the rotor and will be less stable if the discs are placed more towards the centre of the rotor. It is due to the gyroscopic stiffening of the rotor. This stiffening effect will be less when the discs are towards the centre of the rotor.

Case study analysis

For the steady-state harmonic response, we analyze each harmonic independently. The steady-state responses for the 4× and 8× are shown in Figure 6.5-13. The total response is the vector summation of these two responses. The resonance (critical) speeds can also be found using critical speed analysis by specifying the different spin/whirl ratio for different harmonics. The first critical speed due to 4× excitation can be calculated by specifying the spin/whirl ratio of 0.25=1/4 (4 ω ω= = Ω exc) in the critical speed analysis. When the system natural frequency equals the excitation frequency, which is four times the rotor speed, resonance occurs. As calculated and noted in Figure 6.5-14, a rotor speed of 1,385 rpm excites the first natural frequency of 5,541 rpm (92 Hz). Therefore, the rotor speed of 1,385 rpm is the critical speed for the 4× harmonic excitation. Note that due to the damping effect, the peak response occurs slightly higher than the calculated critical speed. By specifying different spin/whirl ratios, critical speeds for other harmonics can also be calculated, e.g., a spin/whirl ratio of 0.125 for the 8× harmonic excitation.

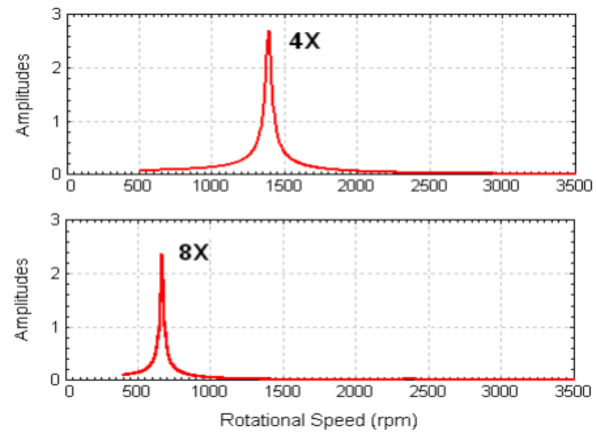

Steady-state response for 4× and 8× harmonics in vertical direction

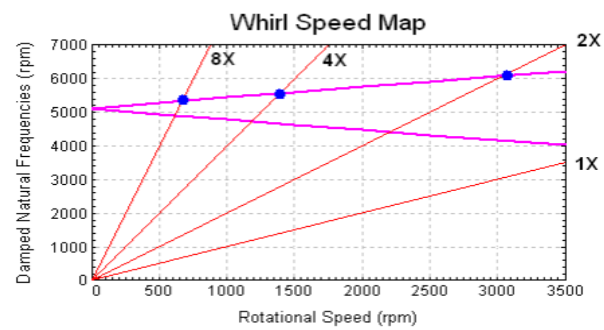

Whirl Speeds and Stability After discussions of the critical speeds and steady-state response, now let us examine another important design consideration: system stability. Rotor stability is a vital characteristic for smooth operations in many high-speed turbomachinery applications. Most turbomachinery is operated in the stable regime based on linear theory; however, for very high-speed and light-weight applications (e.g., the automobile turbochargers) and vertical rotor applications, it is possible to operate the units in the unstable regime defined and predicted by linear theory. In rotordynamics analysis, rotor stability is determined by using the real part of the system's eigenvalue. The eigenvalue for each vibration mode at a specified rotational speed takes the form:

$$\lambda = \sigma \pm j\omega_d = -\xi\omega_n \pm j\omega_n\sqrt{1-\xi^2}$$

where

λ = system eigenvalue

σ = system damping exponent, $\sigma = -\xi\omega_n$

ω_d = damped natural frequency (whirl frequency), $\omega_d = \omega_n\sqrt{1}$

ω_n = undamped natural frequency, $\omega_n = \dfrac{\omega_d}{\sqrt{1-\xi^2}}$

ξ = damping factor (ratio), $\xi = \dfrac{-\sigma}{\omega_n}$

They are also referred to as the whirl speeds or whirl frequencies. If the damped natural frequency is a positive value, this mode is referred to as a precessional mode with an oscillating frequency that equals the damped natural frequency. If the damped natural frequency equals zero, this mode is referred to as a real mode or nonoscillating mode. The real parts of the eigenvalues σ are the system damping exponents, which are used to determine system stability in the linear sense. A positive damping exponent (σ), which is a negative damping factor (ξ), indicates system instability. The associated eigenvectors define the mode shapes for the processional modes, for which the rotor system will vibrate at resonance when damping is not present. The magnitude of the damping factor can also be used to determine whether the transient motion is stable or unstable, oscillatory or non-oscillatory. When the damping factor is less than zero (ξ < 0), the transient motion is exponentially increasing with time, and the system is said to be unstable in linear theory. Eventually, the motion will be constrained in a limit cycle motion through use of non-linear theory, and linear theory does not apply in this regime of operation. In practice, the motion will be restrained in an acceptable limit cycle, or contact will occur and machine parts will be damaged. For the stable and underdamped case (0 1 > ξ >), the transient motion is oscillatory with a decaying amplitude and an oscillating frequency of ωd . For the overdamped case (1 ξ >), the transient motion is non-oscillatory with an exponentially decaying function of time. For the critically damped case (1 ξ =), which separates the underdamped (oscillatory) and overdamped (non-oscillatory, aperiodic) cases, the transient motion is non-oscillatory and the amplitude decays faster than in any other cases. Another quantity commonly used in the study of system stability is the logarithmic decrement. The logarithmic decrement is a measure of the rate of decay or growth of free (transient) oscillations, and is defined as the natural logarithm of the ratio of any two successive amplitudes,

$$\delta = \ln\left(\frac{x_i}{x_{i+1}}\right)$$

where 1 , i i+ x x are two successive transient vibration amplitudes. A negative logarithmic decrement indicates that the transient motion is exponentially growing and the system is unstable in the linear sense. The logarithmic decrement for a precessional mode can be expressed by using the eigenvalue as:

$$\delta = \frac{-2\pi\sigma}{\omega_d} = \frac{2\pi\xi}{\sqrt{1-\xi^2}}$$

The logarithmic decrement can be obtained by measurement and, once it is known, the damping ratio can be obtained from the following equation:

$$\xi = \frac{\delta}{\sqrt{4\pi^2+\delta^2}}$$

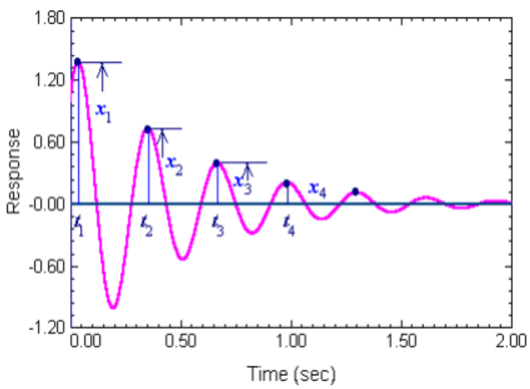

Definition of logarithmic decrement

For very lightly damped system (damping factor 1 ξ <<), the amplification factor defined from the steady-state response curve and the damping factor derived from the whirl speed analysis are related by the following approximation

$$AF = \frac{N_{cr}}{N_2 - N_1} \approx \frac{1}{2\xi}$$

This shows that the amplification factor AF is inversely proportional to the damping factor ξ in very lightly damped systems. It indicates that higher damping results in a lower amplification factor. Figures 6.6-2 and 6.6-3 show both the amplification factor and logarithmic decrement vs. the damping factor for the steady-state unbalance response of a single DOF system and defined by the API specifications, if the amplification factor at a particular critical speed, as measured at the vibration probe, is less than and logarithmic decrement, we know that if the logarithmic decrement is greater than 1.11 or the damping factor is greater than 0.17, the system is said to be a "critically damped" system.

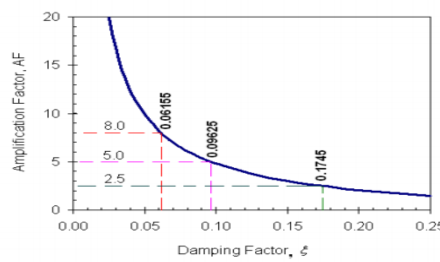

Amplification factor vs. damping factor

Logarithmic decrements and damping factors at three amplification factors

Amplification Factor	Damping Factor	Logarithmic Decrement
2.5	0.17450	1.11350
5.0	0.09625	0.60758
8.0	0.06155	0.38746

The damped natural frequencies and associated normal precessional modes are numbered 1B, 1F, 2B, 2F, etc. The numeric values (1, 2, 3, etc.) represent the mode numbers, which are ordered according to the values of the damped natural frequencies. The letters B and F indicate the directions of the rotor's precession. "B" denotes the backward whirl and "F" denotes the forward whirl. At zero speed, the forward and backward natural frequencies are the same (repeated eigenvalues), and the associated planar modes vibrate in the X and Y directions, respectively. These two modes split into two curves as the rotor speed increases, and the two planes of motion are coupled due to the gyroscopic effect. As the speed increases, the forward whirl frequencies that has damped backward synchronous critical speeds. Caution must be taken when using this whirl speed map to determine the locations of the critical speeds, however, because the peak response very often does not occur at the analytical resonance frequency due to the system complexity.

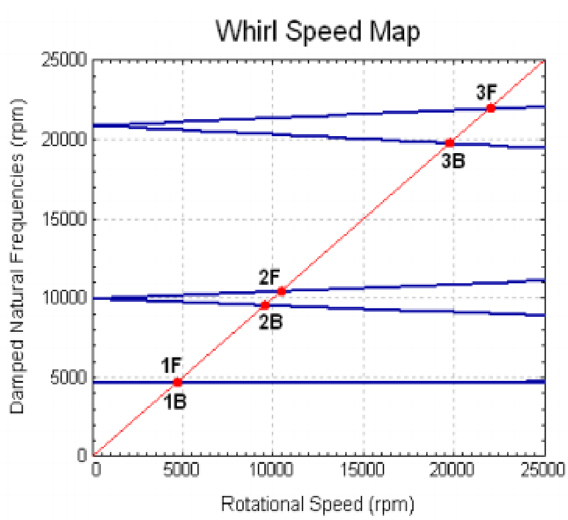

Whirl speed map

Without any destabilizing forces included in the model, all the modal damping factors are positive, as shown in the stability map which indicates that all the precessional modes are stable. Again, the mode numbers are ordered according to the values of the damped natural frequencies. At rotor speeds less than 6,000 rpm, the first backward mode has the lowest damping factor; as the speed increases and exceeds 6,000 rpm, the damping factor of the third forward mode (first bending mode) decreases quickly with the speed and has the lowest value. Note that in this example no any destabilizing forces are applied in the model; the damping factor of the first forward mode actually increases slightly as the speed increases, which is not typical for systems with fluid film bearings. Systems with destabilizing forces will be discussed later. The mode shapes for the first six modes (three backward and three forward) at a rotor speed of 3,575 rpm are plotted.

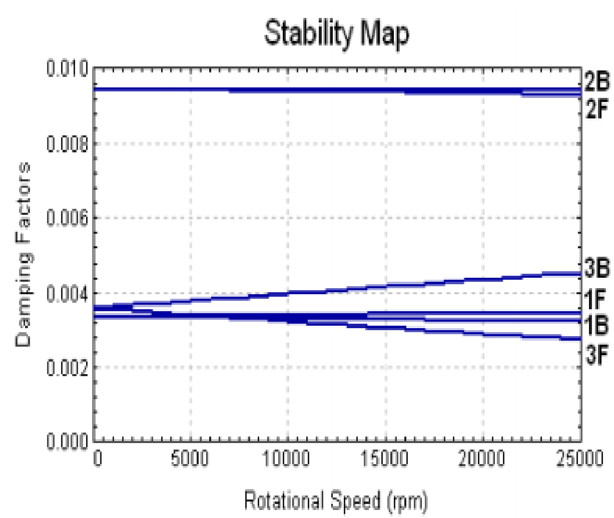

Stability map

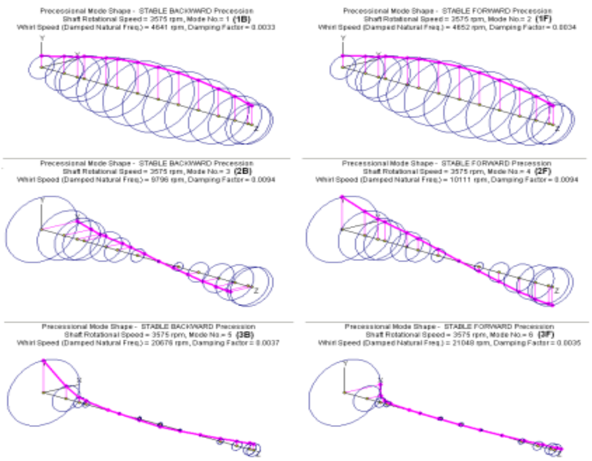

Mode shapes for the first six modes at 3,575 rpm

It plots the imaginary part of the eigen values (frequency) vs. the real part of the eigenvalues (damping exponent) for a range of rotor speeds. Again, the first forward precessional mode becomes unstable when rotor speed exceeds 8,375 rpm. The root locus plot is not commonly used in rotor dynamics study, since the instability threshold speed is not as apparent as in the stability map, where the speed is labeled in the X-axis. It is more widely used in control theory

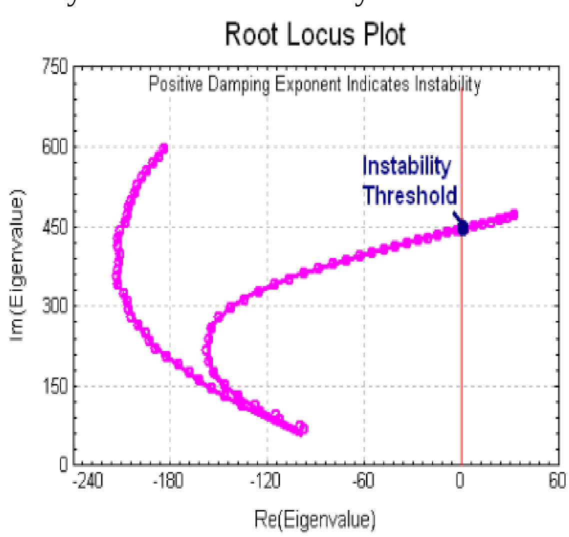

Root locus plot

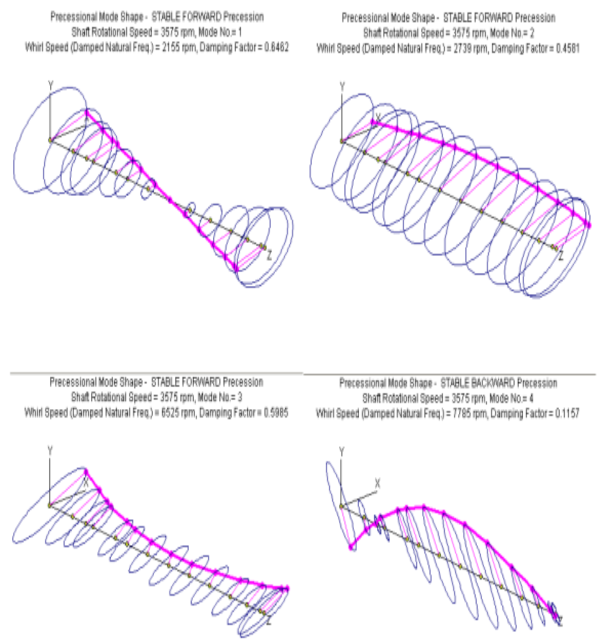

Mode shapes for the first four modes at 3,575 rpm

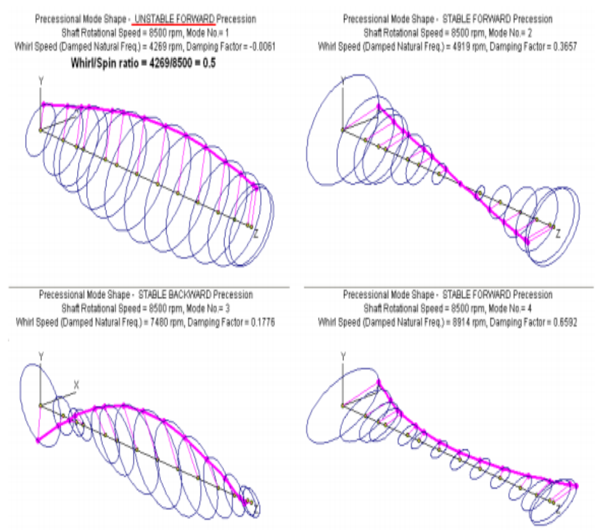

Mode shapes for the first four modes at 8,500 rpm

In addition to the destabilizing forces from the cross-coupled stiffness coefficients of fixed-profile fluid film journal bearings, other destabilizing mechanisms are present in rotating machinery, such as aerodynamic forces caused by the impeller clearance cross-coupling will be used to illustrate their effect. The aerodynamic cross-coupling force induced by the working fluid destabilizes the rotor system. For simplicity, let us add the same magnitude of destabilizing aerodynamic cross-coupled stiffness (Q = Kxy = −Kyx) in all six impellers to study the rotor stability at its normal operating speed of 3,575 rpm. The system studied here is a system with identical roller bearings (K=5.0E05 Lbf/in and C=10 Lbf-s/in), which have limited damping. In this configuration, the only destabilizing forces are the aerodynamic cross-coupling forces, and the system is isotropic with circular orbits. The damping factors for the first six modes (three forward and three backward) vs. the aerodynamic cross-coupling Q at the design speed of 3,575 rpm are tabulated

Q	First Backward ω_d=4641	First Forward ω_d=4652	Second Backward ω_d=9796	Second Forward ω_d=10111	Third Backward ω_d=20676	Third Forward ω_d=21048
0	0.0033	0.0034	0.0094	0.0094	0.0037	0.0035
500	0.0056	0.0011	0.0097	0.0091	0.0038	0.0034
700	0.0065	0.0002	0.0099	0.0090	0.0038	0.0034
750	0.0068	**-0.0001**	0.0099	0.0090	0.0038	0.0034
1000	0.0079	**-0.0012**	0.0100	0.0088	0.0038	0.0034

Damping factors vs. aerodynamic cross-coupling Q at 3,750 rpm

The results show that the cross-coupled stiffness has little effect on the natural frequencies of this isotropic system. However, it affects the damping factors (system stability). The cross-coupled stiffness destabilizes the forward circular modes and stabilizes the backward circular modes. In this example, the aerodynamic cross-couplings have little influence on the third mode due to little modal displacement at the impeller locations, as shown in the mode shape plot.

The damping factor of the first forward mode decreases rapidly as the aerodynamic cross-coupled stiffness Q increases, and this mode becomes unstable when Q exceeds 750 Lb/in. It is important to note that the unstable whirling frequency caused by the aerodynamic crosscoupled stiffness in this example is 4,652 rpm, which is higher than the rotor speed of 3,575 rpm. This differs from the oil whirl frequency caused by the fluid film bearings, which is around half the rotor speed. For this six-stage compressor with fluid film bearings (damping in the range of 1,700- 3,900 Lbf-s/in), it will take as much as 115,000 Lbf/in aerodynamic cross-coupling Q at all impeller stations to destabilize the rotor system, which is more than 150 times that for roller bearings.

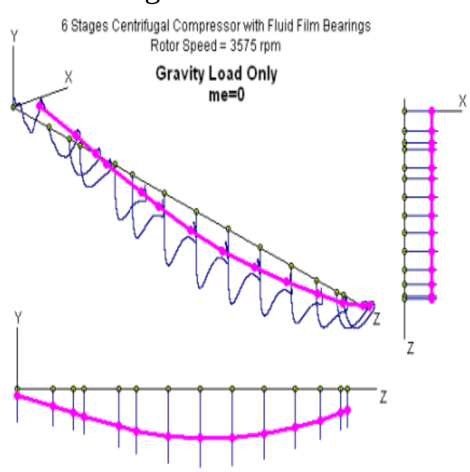

Static deflection curve from transient

analysis

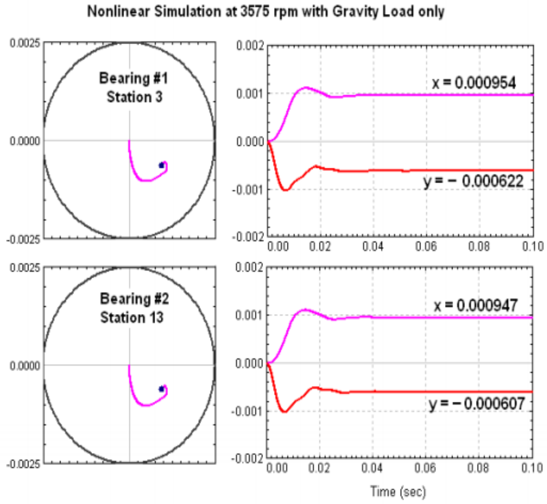

Bearing equilibrium position – nonlinear analysis

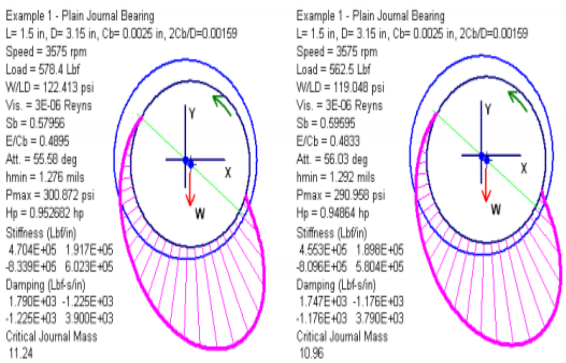

Bearing equilibrium position – Reynolds equation

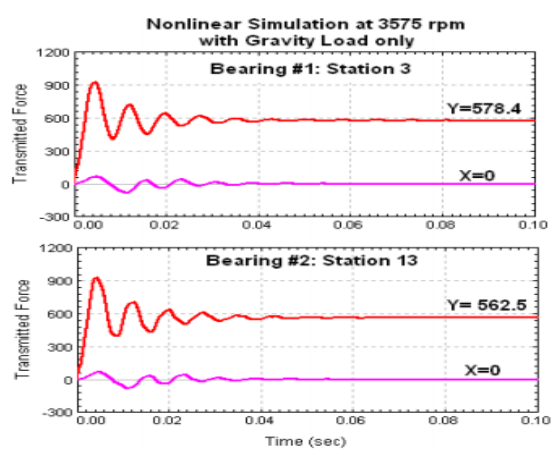

Bearing reaction force

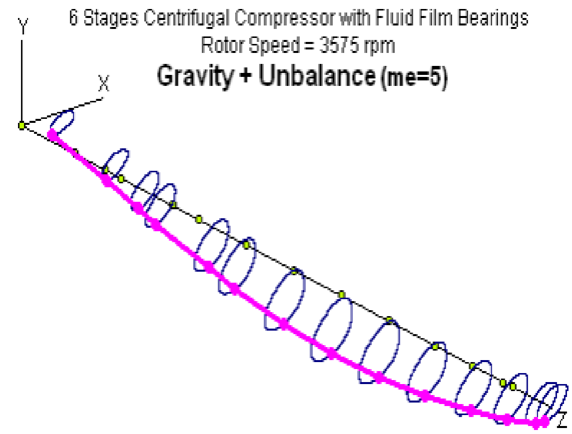

Rotor steady-state response with gravity and unbalance force at a speed below the instability threshold

The rotor responses at bearings for various unbalance forces. It shows that for small amounts of unbalance, the response orbit is around the static equilibrium position (me=0) and nearly elliptical. As the unbalance increases, the response orbit increases. However, the orbit size does not increase linearly with unbalance force as linear theory predicts. In the non-linear systems, the relationship between the unbalance force and response is no longer linear, as illustrated . The FFT analysis shows that the response under unbalance excitation is mainly whirling at 3,575 rpm, which is synchronous with the rotor speed. This synchronous vibration is commonly referred to as "1×" vibration. As the response orbit increases with unbalance, 2× and higher harmonic vibration components show up and the elliptical orbit distorts, as illustrated.

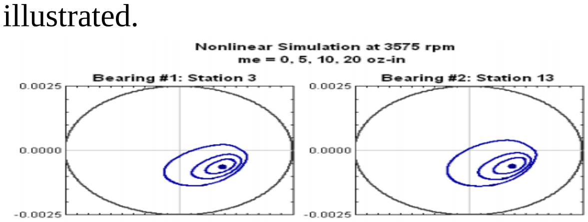

Bearing steady-state response – nonlinear simulation

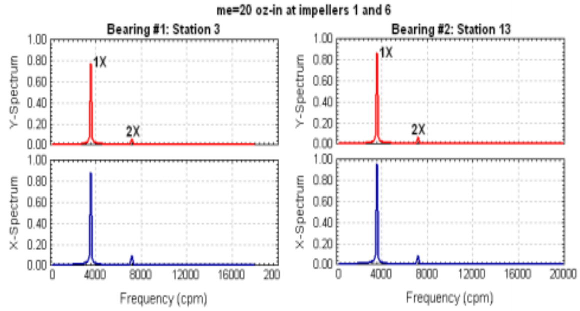

Rotor response spectra at bearings

This beating phenomenon occurs only in lightly damped systems. Although shortening the startup time can lower the peak amplitude when moving through the critical speeds, it is not a good practice for lightly damped systems, because the rotor will also coast down (decelerate) through the critical speeds. For gear-driven machines, shortening the startup time indicates that a large startup torque is required. This could cause damage in the coupling and shaft due to high torque (stress) during startup.

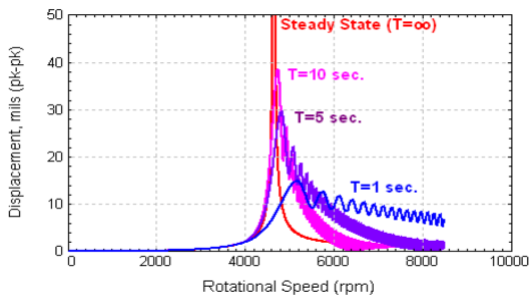

Acceleration effect

The maximum amplitude for the synchronous vibration occurs around 6,500 rpm where the critical speed is located. The sub-synchronous vibration occurs around 8,000 rpm and intensifies after 8,500 rpm.

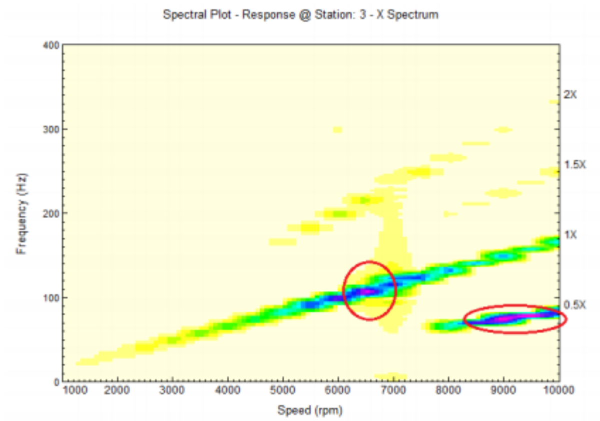

Spectral intensity plot

CONCLUSIONS

The aim of this project is to gain insight into the gyroscopic effects on the rotor disc system. For this purpose mathematical model of the system is used to study its stability. Furthermore, optimisation techniques are utilised in order to ensure high stability of the system under working conditions. The main concentration was speed of the system as nowadays high speed rotors are of prime importance because of the need for speedy works.

A literature survey has been carried out to investigate the developments in modelling and optimisation techniques. It is observed that a huge amount of work has been done in modelling different kinds of rotor with bearings. Most of them involved the Finite Element Modelling. It was also, observed that a number of researchers have used different optimisation techniques with different objective functions in order to make rotor systems stable. However, the existing literature fails to give us a technique that can be combined readily with today's advanced computation techniques and easy to handle both linear and non-linear systems. As a consequence, it was decided to work on some technique that can fulfil the required need.

Here, this work gives the equations of motion of a viscoelastic rotor-shaft system. The linear viscoelastic rotor-material behaviour is represented in the time domain where the damped shaft element is assumed to behave as Voigt model. The finite element model is used to discretize the continuum which is based on Euler-Bernoulli beam theory. Use of LMI technique has been shown here to optimize disc dimension for high dynamic performance of the rotor shaft system. The advantage of the proposed method is the flexibility offered by the LMI formulation, which can be used to create design specifications concerning vibration amplitudes, stability, critical speeds, modal damping levels, and parameter constraints. This work also includes the effects of disc positions in a rotor system. Results are obtained for different sets of disc positions to study the dynamic characteristics, where stability limit of spin speed and unbalance response amplitude are two indices. The rotor will be more stable if the discs are placed towards the ends of the rotor and will be less stable if the discs are placed more towards the centre of the rotor. Thus, proper placement of disc together with optimized dimensions will ensure high stability and less response amplitude.

For more accurate results, normally about one-tenth of the maximum suggested time step is recommended in the numerical simulation. Thus, Δt = 1E-05 is used for linear problems in the above example. For nonlinear problems, a smaller time step is necessary for the solution to converge. Typically, Δt = 1E-06 is suggested for nonlinear problems. For highly nonlinear systems, such as automotive turbochargers, a further smaller time step is required for solution convergence.

REFERENCES

[1] Boyd, S., Ghaoui, L. EI, Feron, E. and Balakrishnan, V., 1994, *Linear Matrix Inequalities in system and control theory*, SIAM, Philadelphia.

[2] Gahinet, G., Nemirovski, A., Laub, A. J. and Chilai, M., 1995, *LMI control toolbox*, The Mathworks, Inc..

[3] Genta, G., 1999, *Dynamics of rotating systems*, Springer Verlag.

[4] Lalanne, M. and Ferraris, G., 1998, *Rotor dynamics prediction in engineering*, John Wiley and Sons.

[5] Rao, J. S., 1996, *Rotor dynamics*, New Age International Publishers.

[6] Stodola, A., 1927, Steam and gas turbines, McGraw-Hill, New York.

[7] Kandil, M. A., 2004, "*On rotor internal damping instability*", Doctoral thesis,Department of Mechanical Engineering, Imperial College of London.

[8] Dickmen, E., 2010, "Multiphysical effects on high-speed rotordynamics", Doctoral Thesis, University of Twente, Enschede, Netherlands.

[9] Belluzzo, G., 1905, "Le turbine a vapore ed a gas", Hoepli, Milano, Italy.

[10]Bhavikatti, S. S. and Ramakrishnan, C. V., 1980, "Optimum shape design of rotating discs", *Computers and Structures*, Pergamon Press Ltd, **11**, pp. 377-401.

[11] Bulatovic, R. M., 1999, "A stability theorem for gyroscopic systems", *Acta Mechanica*, **136**, pp. 119-124.

[12] Bulatovic, R. M., 2001, "Condition

for instability of conservative gyroscopic systems", *Theoretical and Applied Mechanics*, **26**, pp. 127-133.

[13] Bulatovic, R. M., 2001, "On the Lyapunov stability of linear conservative gyroscopic systems", *C.R. Acad. Sci., Paris*, **324**, pp. 679-683.

[14] Bulatovic, R. M., 1997, "The stability of linear potential gyroscopic systems when the potential energy has a maximum", *Journal of Applied Mathematics and Mechanics*, **61**, pp. 371-375.

[15] Cao, Y. Y., Lam, J., Sun, X. Y., 1998, "Static output feedback: An ILMI approach", *Automatica*, **34** (12), pp. 1641-1645.

[16] Chen, T. Y., and Wang, B. P., 1993, "Optimum design of rotor-bearing system with eigenvalue constraints", *Journal of Engineering for Gas Turbines and Power*, **115**, pp. 256-260.